Nuclear Inst. and Methods in Physics Research, A 887 (2018) 54–58

Contents lists available at ScienceDirect

Nuclear Inst. and Methods in Physics Research, A

journal homepage: www.elsevier.com/locate/nima

A flexible, on-line magnetic spectrometer for ultra-intense laser produced fast electron measurement

Xulei Ge [a,b,c], Xiaohui Yuan [b,c,*], Su Yang [b,c], Yanqing Deng [b,c,d], Wenqing Wei [b,c], Yuan Fang [b,c], Jian Gao [b,c], Feng Liu [b,c,*], Min Chen [b,c], Li Zhao [a], Yanyun Ma [c,d], Zhengming Sheng [b,c,e], Jie Zhang [b,c]

[a] State Key Laboratory of Surface Physics and Department of Physics, Fudan University, Shanghai 200433, China
[b] Key Laboratory for Laser Plasmas (Ministry of Education) and School of Physics and Astronomy, Shanghai Jiao Tong University, Shanghai 200240, China
[c] Collaborative Innovation Center of IFSA (CICIFSA), Shanghai Jiao Tong University, Shanghai 200240, China
[d] College of Science, National University of Defense Technology, Changsha 410073, China
[e] SUPA, Department of Physics, University of Strathclyde, Glasgow G4 0NG, UK

ARTICLE INFO

Keywords:
Electron spectrometer
On-line spectrometer
Ultra-intense laser-solid interaction

ABSTRACT

We have developed an on-line magnetic spectrometer to measure energy distributions of fast electrons generated from ultra-intense laser-solid interactions. The spectrometer consists of a sheet of plastic scintillator, a bundle of non-scintillating plastic fibers, and an sCMOS camera recording system. The design advantages include on-line capturing ability, versatility of detection arrangement, and resistance to harsh in-chamber environment. The validity of the instrument was tested experimentally. This spectrometer can be applied to the characterization of fast electron source for understanding fundamental laser-plasma interaction physics and to the optimization of high-repetition-rate laser-driven applications.

1. Introduction

The interaction of ultra-intense laser with overdense plasma produces large-current relativistic (fast) electron beams. Knowing the electron energy distribution and its dependence on laser and target parameters are important to the understanding of fundamental laser-plasma physics, and to the optimization of electron sources for applications, e.g., the fast ignition (FI) [1] approach to inertial confinement fusion (ICF), laser-driven ion acceleration [2,3] and bright radiation sources development [4,5].

The electron energy spectrum is normally measured with a dipole magnet based electron spectrometer. The electrons are first dispersed according to the different kinetic energies in the magnetic field and then recorded by the detector(s). Three major detection methods previously reported are image plates (IPs), scintillating fibers and scintillator screen both imaged directly with CCD/sCOMS camera. The major drawback of IPs [6,7] is the need to vent the vacuum chamber to read the stored signals. Therefore IPs are not appropriate for high-repetition-rate experiments. The scintillator fibers [8–11] are normally placed parallel to the magnetic lines along the sides of both plates. The effects of fringe field on electron deflection trajectory are inevitable [12]. In addition, the effective fiber length which produces scintillating light is only a small portion of the fiber. The longer redundant fibers beyond the magnetic field region will produce background scintillating light when exposed to optical light or particles. To eliminate the undesired background, Chen et al. [10] has put the CCD camera inside the vacuum chamber to shorten the fiber length. However, the CCD suffered from the strong electromagnetic pulses (EMP) [13] in the harsh environment and may not work properly [14]. When scintillator screens [15–18] were used, they were normally imaged directly with an optical lens coupled CCD camera. Extensive shielding is an essential requirement to avoid scattered optical light entering the imaging system. Due to the large aspect ratio of screen (> 10) and considerable length along the dispersion direction (normally tens of centimeters), effectively only a very small portion of CCD chip was used, limiting the spatial resolution on the scintillator detector by the imaging system to only several hundred microns [2]. Another important issue is that the imaging system needs be realigned when changing the positions of the electron spectrometer to measure electron spectra along other directions.

* Correspondence to: Key Laboratory for Laser Plasmas (Ministry of Education) and School of Physics and Astronomy, Shanghai Jiao Tong University, 800 Dongchuan Rd. Minhang District, Shanghai 200240, China.
E-mail addresses: xiaohui.yuan@sjtu.edu.cn (X. Yuan), liuf001@sjtu.edu.cn (F. Liu).

https://doi.org/10.1016/j.nima.2017.12.054
Received 25 July 2017; Received in revised form 15 December 2017; Accepted 16 December 2017
Availableonline 8 January 2018
0168-9002/

In this paper, we present a novel design of a flexible, on-line magnetic spectrometer, which utilizes the scintillator screen to produce scintillating light and employs the non-scintillating fibers to guide light to high frame-rate sCMOS camera imaging system. This instrument combines the advantages of the on-line capability of scintillator, flexibility and versatile transforming configuration of the fibers, and resistance to harsh environment by moving the recording electronics out of the vacuum chamber.

2. Spectrometer design

The schematic of the spectrometer is shown in Fig. 1(a) (the imaging system is not presented). A pair of parallel NdFeB permanent magnets, shown in light blue, deflects the electrons according to their different kinetic energies (representative lines in black). A thin sheet of plastic scintillator (in dark red) is inserted inside the magnetic spectrometer to convert the electron signal into visible optical light. The scintillator screen can facilitate an on-line detection capability since the emitted light from the scintillator can be captured by the imaging system without disturbing the detector. This would attract more interests especially in high-repetition-rate single-shot evaluations for statistical analysis.

A bundle of fibers, arranged in multiple rows of linear arrays, are placed with one end in close contact with the scintillator sheet. The light signals from the scintillator are then relayed by the fibers to the imaging system placed outside the vacuum chamber [19]. A high frame-rate sCMOS camera located outside the vacuum chamber is used to record the optical light transmitted through a glass window. Considering the aspect ratio of sCMOS chip size, the other end of the fiber bundle is rearranged to an areal configuration. The insets in Fig. 1(a) illustrate the linear and areal interfaces of the fiber bundle, respectively. A photo of the assembly is shown in Fig. 1(b).

Trapezoidal-shaped (truncated square) magnets (marked by dashed-line in Fig. 2(a)) are used in this work. The magnet plates have an overall side-length of 200 mm and a separation gap of 10 mm. They are enclosed with a 10-mm-thick iron yoke. The spatial distribution of the magnetic field strength in the mid-plane was mapped out with a Hall probe, and is shown as the grayed area in Fig. 2(a). The peak field strength is 0.12 T. The fringed field decreases from 0.10 T at the edge to 0.05 T 10 mm away from the magnet plates. If the detector is not inside the uniform region and there is no collimator at the entrance, the electron trajectories and energy dispersions need to be precisely simulated using a particle tracing program [12] in order to include the effects of fringe fields. Simplified calculations using simple Lorentz force consideration can be obtained by minimizing fringe field effects with a collimator placed inside a central region of 160 mm with field strength variation of only 1.26% (standard deviation). An ultralow-carbon stainless-steel collimator was chosen as the entrance. The collimator is 30 mm long with a 3.5 mm hole in the center (yellow in Fig. 2(a)). The magnetic field increases from 0 to 0.12 T within 13 mm beyond the collimator hole. The scintillator screen was also inserted into the near-uniform magnetic field region further reducing the effect of fringe field. A visible CW laser (red dash line) was used to align the spectrometer.

The plastic scintillator is a DRZ fluorescent screen (Gd_2O_2S:Tb, type Pl-200) having dimensions of 200 mm (length) × 10 mm (width) × 630 μm (thickness) and emits light at 546 nm when impacted by energetic electrons. The scintillator screen itself has a higher spatial resolution (a few 10's of microns) than the large-diameter scintillator fibers (typical 500 μm) [10] and it is not the limiting factor for the energy resolution. A 2 μm-thick aluminum-anodized mylar film was placed before the scintillator to block scatted light. This type of scintillator has been calibrated using ultrashort electron beam from a radio frequency linear electron accelerator [20]. The 20 cm-long plastic scintillator sheet (dark-red line in Fig. 1(a)) was positioned at 45° with respect to the entrance axis. In this case, the spectrometer works in the focusing mode, i.e. finite-diameter collimated electron beam is bent by the magnet and overlaps on the detector plane [11]. The corresponding trajectories of

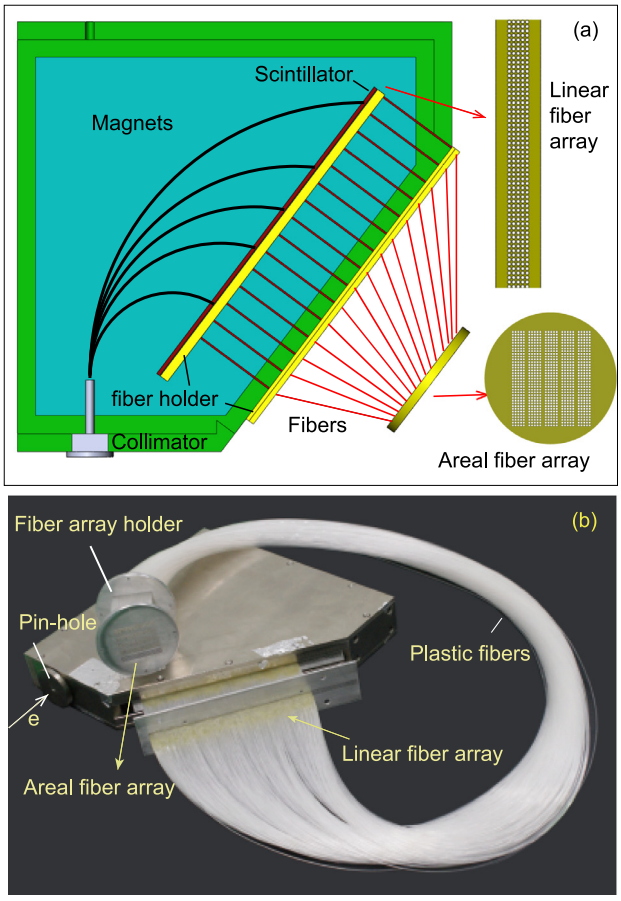

Fig. 1. (Color online) The schematic (a) and photograph (b) of the magnetic spectrometer. The regions in light blue and in green are magnet plates and the yoke, respectively. A collimator was inserted into the region of near-uniform magnetic field strength. The red lines indicate the fiber bundles. Two insets in (a) show the linear and areal interfaces of the fiber bundle.

the electrons with different energies were computed by calculating the deflection angle according to the Lorentz force, which are shown in Fig. 2(a).

A total number of 875 equally spaced 1 m-long plastic fibers are placed in close contact with the scintillator, to sample and guide the optical light signals out of the spectrometer. The fiber bundle was further wrapped with aluminum to avoid stray light. The cross-talk between channels was also checked using a point laser source to be <4%. Although the spatial resolution of the non-scintillating fibers is not as high as that of IPs, they were chosen due to several advantages. Firstly, it is easier to shield the imaging system from scattered lights, and no optics are required in the crowded chamber, saving space for other diagnostics. Secondly, the fibers can be easily bent. Therefore, the imaging system can be set up using chamber windows away from the influences of radiations (especially EMPs) and also to avoid conflicts with other diagnostics. Thirdly, the plastic fibers can be rearranged into a matrix to fit the sCMOS/CCD camera sensor for better imaging. Fourthly, the imaging component does not require alignment, when re-positioning of the main body of the spectrometer becomes necessary to measure the electron spectra along other directions. Lastly, the fibers are insensitive to the radiations, hence no extensive shieldings are needed.

Each fiber has a diameter of 0.75 mm. The separation of the centers of adjacent fibers is 1 mm. In the scintillator end, five fibers were employed in the non-dispersion direction for each specific electron energy, thus forming a matrix of 5 × 175 fibers. This gives rise to 175 energy points in the dispersion direction. Fig. 2(b) shows the energy